

# Magnetic properties of DyMn<sub>6</sub>Ge<sub>6</sub> studied by neutron diffraction and magnetic measurements

P. Schobinger-Papamantellos\*

*Institut für Kristallographie und Petrographie, ETH Zürich, CH-8092 Zürich (Switzerland)*

F.B. Altorfer

*Labor für Neutronenstreuung ETHZ-PSI, CH-5232 Villigen PSI (Switzerland)*

J.H.V.J. Brabers and F.R. de Boer

*Van der Waals-Zeeman Laboratory, University of Amsterdam, NL-1018 XE Amsterdam (Netherlands)*

K.H.J. Buschow

*Philips Research Laboratories, NL-5600 JA Eindhoven (Netherlands)*

(Received July 4, 1993)

## Abstract

The compound DyMn<sub>6</sub>Ge<sub>6</sub> crystallizes in the hexagonal HfFe<sub>6</sub>Ge<sub>6</sub>-type structure (*P6/mmm*). It orders antiferromagnetically at  $T_N = 420$  K but there is a second magnetic phase transition near 100 K. Neutron diffraction has shown that the high temperature magnetic structure is a triple flat spiral consisting of ferromagnetic Dy layers and ferromagnetic Mn layers coupled antiparallely in a three-layer sequence Mn(+), Dy(-), Mn(+). The moment direction is perpendicular to [001] but the direction in the basal plane changes by a constant angle  $\phi_s = 2\pi q_x$  on going from one unit cell to another. The wavevector length of the incommensurate structure is temperature dependent and equal to  $q_x = 0.184$  at 293 K, which corresponds to  $\phi_s = 66^\circ$ . Below  $T_i = 100$  K the wavevector length remains constant ( $q_x = 0.163$ ) and the magnetic structure is an incommensurate triple-cone structure in which both the Dy and Mn sublattices have a ferromagnetic component along the *c* axis. These components are antiparallel and lead to a net moment in the *c* direction of  $2.0(5) \mu_B$  per formula unit. The magnetic isotherm at 4.2 K, studied in fields up to 35 T, suggests that below 22 T the cone angle ( $55^\circ$  for  $B=0$ ) gradually decreases. Above 22 T the magnetic isotherm shows a linear behaviour characteristic of bending of the antiparallel rare earth and 3d sublattice moments towards each other. The intersublattice coupling constant derived from the high field slope of the isotherm equals  $J_{Dy-Mn}/k = -9.1$  K.

## 1. Introduction

In a previous study [1] we determined the magnetic properties of various compounds of the type RMn<sub>6</sub>Ge<sub>6</sub> (R, heavy rare earth element). Several of these compounds have the interesting property of giving rise to two separate ordering temperatures which were tentatively attributed to antiferromagnetic ordering of the R and Mn sublattices. In GdMn<sub>6</sub>Sn<sub>6</sub> and to some extent also in TbMn<sub>6</sub>Sn<sub>6</sub> we found evidence for an even more interesting magnetic behaviour which we termed bootstrap ferrimagnetism: the antiferromagnetic configurations within both the R and Mn sublattices are simultaneously broken by the R–Mn intersublattice

interaction, leading to a ferrimagnetic alignment of the R and Mn sublattice moments.

In order to obtain more detailed information on the magnetic interactions in this class of materials, we have performed neutron diffraction experiments on DyMn<sub>6</sub>Ge<sub>6</sub>. It will be shown that the magnetic behaviour in DyMn<sub>6</sub>Ge<sub>6</sub> is more complex than a simple combination of two different antiferromagnetic sublattices.

## 2. Sample preparation and magnetic measurements

The DyMn<sub>6</sub>Ge<sub>6</sub> sample was prepared by arc melting from starting materials of at least 99% purity. The sample was wrapped in Ta foil and annealed at 800 °C for 4 weeks in an evacuated quartz tube. After vacuum annealing, the sample was investigated by X-ray diffraction and found to be single phase (HfFe<sub>6</sub>Ge<sub>6</sub> structure type [2, 3]).

\*Permanent guest scientist at the Laboratory for Neutron Scattering, ETHZ-PSI, Villigen, Switzerland.

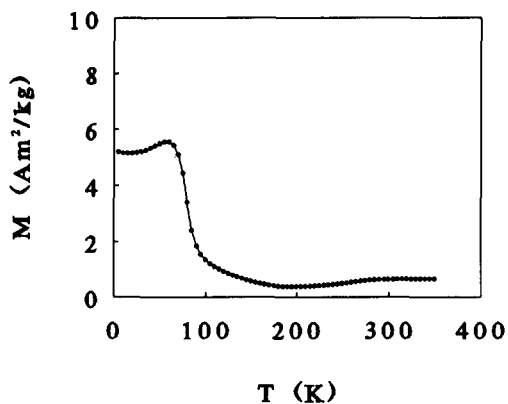


Fig. 1. Temperature dependence of the magnetization of  $\text{DyMn}_6\text{Ge}_6$  measured in a field of 0.1 T.

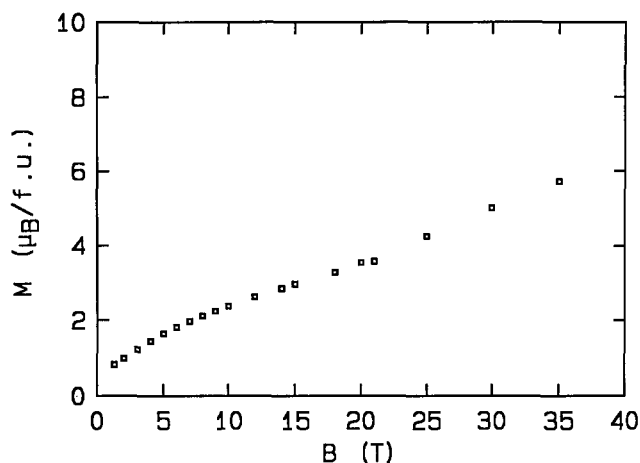


Fig. 2. Field dependence of the magnetization of  $\text{DyMn}_6\text{Ge}_6$  measured at 4.2 K on fine particles able to rotate freely into the equilibrium position under the ambient field strength.

Previous investigations have shown that  $\text{DyMn}_6\text{Ge}_6$  orders antiferromagnetically at about  $T_N = 420$  K [1, 4], as evidenced by a cusp-like peak in the temperature dependence of the magnetization. It was also shown that the magnetization rises again below 100 K with decreasing temperature, leading to a second peak in the temperature dependence of the magnetization at about 70 K [1]. This behaviour is observed also in the present sample, as can be seen in Fig. 1.

The field dependence of  $\text{DyMn}_6\text{Ge}_6$  at 4.2 K was studied on fine powder particles able to rotate freely into the equilibrium position under the ambient magnetic field strength. Results are shown in Fig. 2.

### 3. Neutron diffraction

Neutron diffraction experiments were carried out at the facilities of the Reactor Saphir, Würenlingen in the high temperature (HT) and low temperature (LT)

magnetically ordered states at 293 and 11 K respectively. The data were collected with the "DMC" (double-axis multicounter diffractometer) in the high intensity mode with  $\lambda = 1.7037$  Å. The step increment of the diffraction angle  $2\theta$  was  $0.1^\circ$ . The data were corrected for absorption and evaluated by the FULLPROF program [5] using scattering lengths for Dy, Mn and Ge as reported in ref. 6 and magnetic form factors for  $\text{Dy}^{3+}$  and  $\text{Mn}^{2+}$  as given in refs. 7 and 8 respectively.

#### 3.1. The nuclear structure and the high temperature magnetic structure

The neutron pattern collected in the (HT) magnetically ordered state at 293 K is shown in Fig. 3(a). The refined parameters given in Table 1 confirm the  $\text{HfFe}_6\text{Ge}_6$ -type structure [2, 3]. The  $R$  factors and  $\chi^2$  values are satisfactory and indicate no significant deviation from the basic crystal structure. From the magnetic measurements reported in Section 2 it is expected that magnetic contributions associated with the antiferromagnetic ordering of the Mn sublattices are observed already at room temperature.

In fact, some weak reflections, non-overlapping with the nuclear reflections, are visible in the neutron pattern. The first observable magnetic reflection at  $2\theta = 9.3^\circ$  corresponds to a point within the first Brillouin zone of the chemical cell, indicating that the wavevector of the magnetic structure corresponds to  $\mathbf{q} \neq 0$ . It has been possible to index all magnetic reflections as satellites of the allowed nuclear reflections  $\mathbf{H} \pm \mathbf{q}_z$  (where  $\mathbf{H} = h\mathbf{a}^* + k\mathbf{b}^* + l\mathbf{c}^*$  is a reciprocal lattice vector) using a wavevector incommensurate with the crystal lattice and oriented along the hexagonal  $c$  axis. The wavevector length at 293 K is  $q_z = 0.184(1)$ . Given the fact that only first-order satellites are observed, the magnetic structure may be described by harmonic functions such as a flat spiral or a sinusoidally modulated structure.

Any periodic magnetic moment arrangement with the moments at positions  $\mathbf{R}_{ij} = \mathbf{r}_j + \mathbf{R}_i$ , where  $\mathbf{R}_i = n_1\mathbf{a} + n_2\mathbf{b} + n_3\mathbf{c}$  ( $n_i$  integer) and  $\mathbf{r}_j$  is the position of the  $j$ th atom in the cell, can be described in terms of Fourier expansion series [9, 10] as

$$\begin{aligned} \mathbf{m}_j(\mathbf{R}_i) &= \sum_i \mathbf{m}_j(\mathbf{q}_i) \exp(i\mathbf{q}_i \cdot \mathbf{R}_{ij}) \\ &= \sum_i \mathbf{m}_j(\mathbf{q}_i) \cos(\mathbf{q}_i \cdot \mathbf{R}_j + \phi_{ij}) \end{aligned} \quad (1)$$

In the simple spiral (SS) model the Fourier coefficients can be expressed as a complex vector

$$\mathbf{m}_\mathbf{q} = \frac{m_0}{2} (i\hat{u}_\mathbf{q} + i\hat{v}_\mathbf{q}) \exp(i\phi_\mathbf{q}) \quad (2)$$

where  $\hat{u}_\mathbf{q}$  and  $\hat{v}_\mathbf{q}$  are two orthogonal vectors,  $m_0$  is the moment value and  $\phi_\mathbf{q}$  is the phase factor associated with the wavevector  $\mathbf{q}_i = \mathbf{q}$ . In the model the magnetic

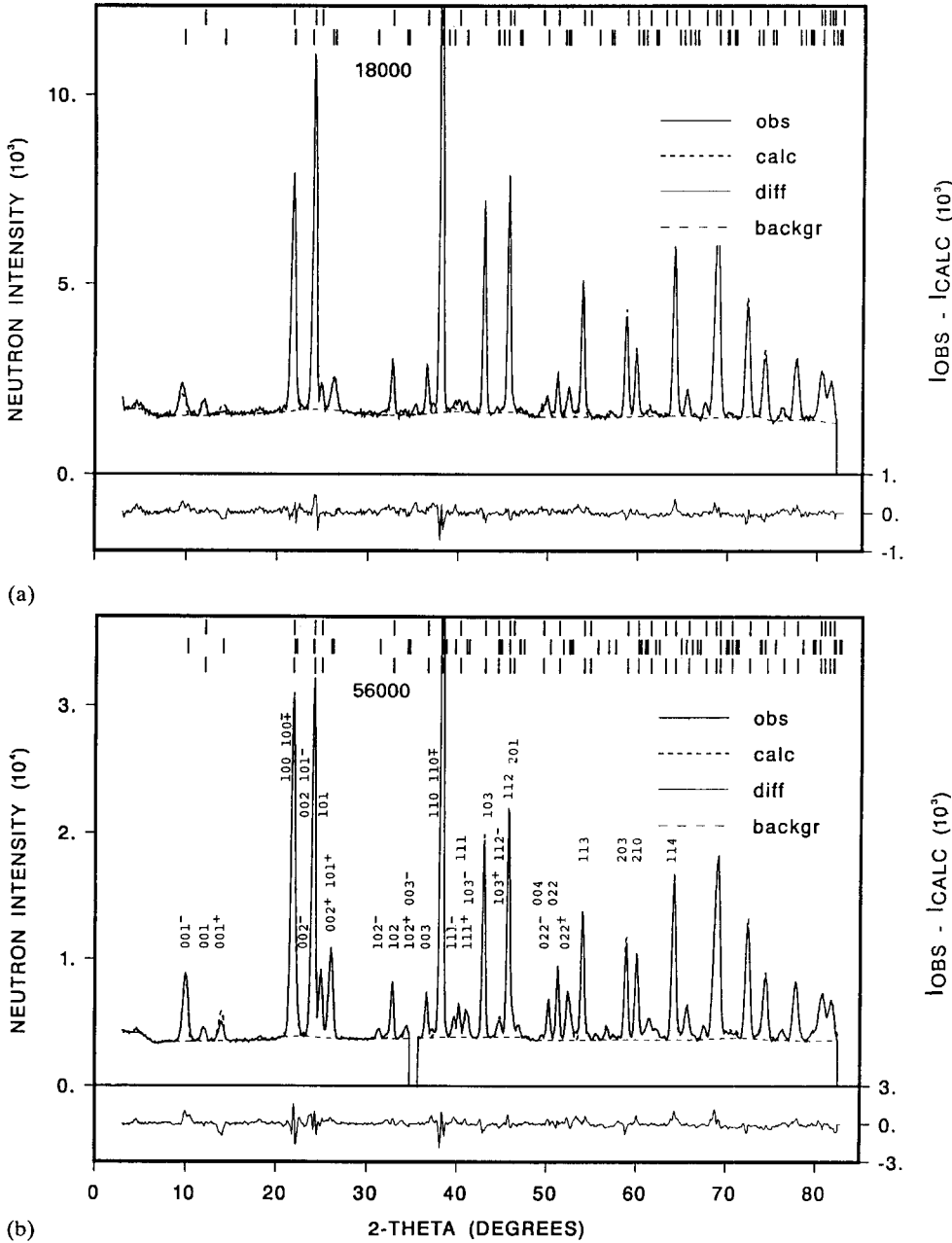


Fig. 3. Observed and calculated neutron diffraction diagrams ( $\lambda = 1.7037 \text{ \AA}$ ) of DyMn<sub>6</sub>Ge<sub>6</sub> at (a) 293 K and (b) 11 K. The difference between observed and calculated intensities is given below each of the diagrams.

moment of the  $j$ th atom in the cell maintains its length but changes its direction by a constant angle  $2\pi q$  on going from one cell to another in the direction of the propagation vector. This angle is usually temperature dependent. The moment distribution in the  $l$ th cell is given by the expression

$$m_l = m_0 [\cos(\mathbf{q} \cdot \mathbf{R}_l + \phi_q) \cdot \hat{u}_q + \sin(\mathbf{q} \cdot \mathbf{R}_l + \phi_q) \cdot \hat{v}_q] \quad (3)$$

where  $m_0$  is the moment value and  $\mathbf{R}_l$  is the position of the  $l$ th unit cell. For a sinusoidally modulated structure the Fourier coefficients are given by

$$m_q = \frac{A_q}{2} \hat{u}_q \exp(i\phi_q) \quad (4)$$

where  $A_q$  is the amplitude of the varying moment component in the direction  $\hat{u}_q$ . The average moment amplitude of an atom varies sinusoidally with the wavevector in the  $l$ th cell, its value being

$$m_l = A_q \cos(\mathbf{q} \cdot \mathbf{R}_l + \phi_q) \cdot \hat{u}_q \quad (5)$$

The refinement made on the basis of the flat spiral model converged by assuming that the magnetic ordering involves both kinds of magnetic atoms (Dy and Mn)

TABLE 1. Refined parameters of DyMn<sub>6</sub>Ge<sub>6</sub> (space group *P6/mmm*) (a) in the HT region, simple spiral (SS) model and (b) in the LT region, ferrimagnetic spiral (FS) model.  $\mu_x$ ,  $\mu_y$  and  $\mu_z$  are the moment components for (i) the spiral, (ii) the ferrimagnetic and (iii) the total of the Dy and Mn sublattices.  $\phi_c$  is the average moment angle with the *c* axis and  $\phi_s$  is the spiral angle associated with the wavevector  $q_z$  (given in reciprocal lattice units *z.l.u.*).  $R_{m1}$  and  $R_{m2}$  are the reliability factors for the integrated magnetic intensities of the spiral and ferrimagnetic structures respectively

Parameter	293 K, SS model	10 K, FS model
Dy at 1b, (0, 0, 0)		
$z_{Mn}$ at 6i, ( $\frac{1}{2}$ , 0, <i>z</i> )	0.2504(6)	0.2503(5)
Ge1 at 2d, ( $\frac{1}{3}$ , $\frac{2}{3}$ , $\frac{1}{2}$ )		
Ge2 at 2c, ( $\frac{1}{3}$ , $\frac{2}{3}$ , 0)		
$z_{Ge3}$ at 2e, (0, 0, <i>z</i> )	0.3453(5)	0.3447(7)
$B_{of}$ (nm <sup>2</sup> )	0.0107(5)	0.0094(5)
$\mu_{xDy}$ , $\mu_{yDy}$ , $\mu_{zDy}$ ( $\mu_B$ )	3.49(8), —, 3.49(8)	5.68(6), 4.01(11), 6.95(5)
$\mu_{xMn}$ , $\mu_{yMn}$ , $\mu_{zMn}$ ( $\mu_B$ )	−1.42(4), —, −1.42(4)	−1.61(2), −1.09(8), −1.94(6)
$\phi_c$ (deg)	90	55(1)
$q_z$ (r.l.u.), $\phi_s$ (deg)	0.184(1), 66.24	0.1631(4), 58.71
<i>a</i> (nm)	0.52262(4)	0.52081(3)
<i>c</i> (nm)	0.81653(6)	0.81522(5)
$R_n$ (%), $R_{wp}$ (%), $R_{m1}$ (%)	4.77, 10.5, 17.3	2.7, 9.6, 11.3
$R_{m2}$ (%), $R_{exp}$ (%), $\chi^2$	4.94, —, 4.94, 4.5, 4.5	3.5, 2.47, 15.1

at 293 K. These moments were found to be coupled antiferromagnetically. The ordered moments within each of the atomic layers of the chemical cell unit point in a common direction parallel to (001). As shown in the top part of Fig. 4(a), the structure consists of a unit of three ferromagnetic Mn(+)Dy(−)Mn(+) layers (at  $z = -\frac{1}{4}, 0, \frac{1}{4}$ ). The moments in this unit collectively change their orientation by 66° within the basal plane on going from one unit cell to another along the direction of the wavevector  $q_z$ , *i.e.* along the *c* direction, as has been indicated schematically in Fig. 4(b). The structure might therefore also be regarded as a triple-spiral structure. The refined moment values of the two sublattices within the hexagonal plane (001) are  $\mu_{xDy} = 3.49(8) \mu_B$  and  $\mu_{yMn} = -1.42(4) \mu_B$ . The absolute moment direction within the hexagonal plane cannot be derived from a powder pattern [11]. Furthermore, since the refined moment values lie below the saturation values of the free ions Mn<sup>2+</sup> and Dy<sup>3+</sup>, one cannot distinguish between a sine-wave-modulated structure and a simple spiral structure. The refined parameters for the former model are given in Table 1. Observed and calculated intensities can be compared with each other in Table 2.

### 3.2. The low temperature magnetic structure

The neutron pattern taken at 11 K comprises two sets of additional reflections associated with the magnetic ordering. For one set the symmetrical distribution of the magnetic satellites on either side of the allowed nuclear reflections (001) and (002) makes it possible to identify it as originating from an incommensurate

wavevector along the *c* axis,  $q_z = 0.1631(4)$ , not much different from that found already for the HT phase. Since only first-order magnetic satellites were observed, the moment arrangement of the LT incommensurate magnetic phase in directions perpendicular to the *c* axis is similar to that of the HT magnetic structure.

The change with temperature in the reflection angle of the most dominant observed magnetic satellites is comparatively small. Also, the intensity ratio ( $I_{001-}/I_{002+}$ ) remains approximately unchanged on going from 293 to 11 K. This indicates that the incommensurate structure remains unchanged with temperature. In fact, it is only the wavevector length that decreases with decreasing temperature and consequently the turn angle within the basal plane direction decreases from 66° at 293 K to 58.68° at 11 K. The intensity increase with decreasing temperature indicates an increase in the planar moment components contributing to the  $m_q$  and  $m_{-q}$  Fourier coefficients.

The second set of additional reflections coincides with the much stronger nuclear reflections ( $q = 0$ ) and is therefore more difficult to detect in the presence of other Fourier coefficients. The existence of magnetic reflections at reciprocal lattice positions ( $q = 0$ ) of the allowed nuclear reflections indicates the presence of ferromagnetic moment components. From the temperature dependence of several of these magnetic reflections, for both sets the direction of the ferromagnetic components was deduced to be along the [001] direction. This results from the temperature dependence of the ratio (001)/(101) of observed intensities at  $2\theta = 12^\circ$  and  $25^\circ$ , which diminishes drastically from 1.35 to 0.35 on

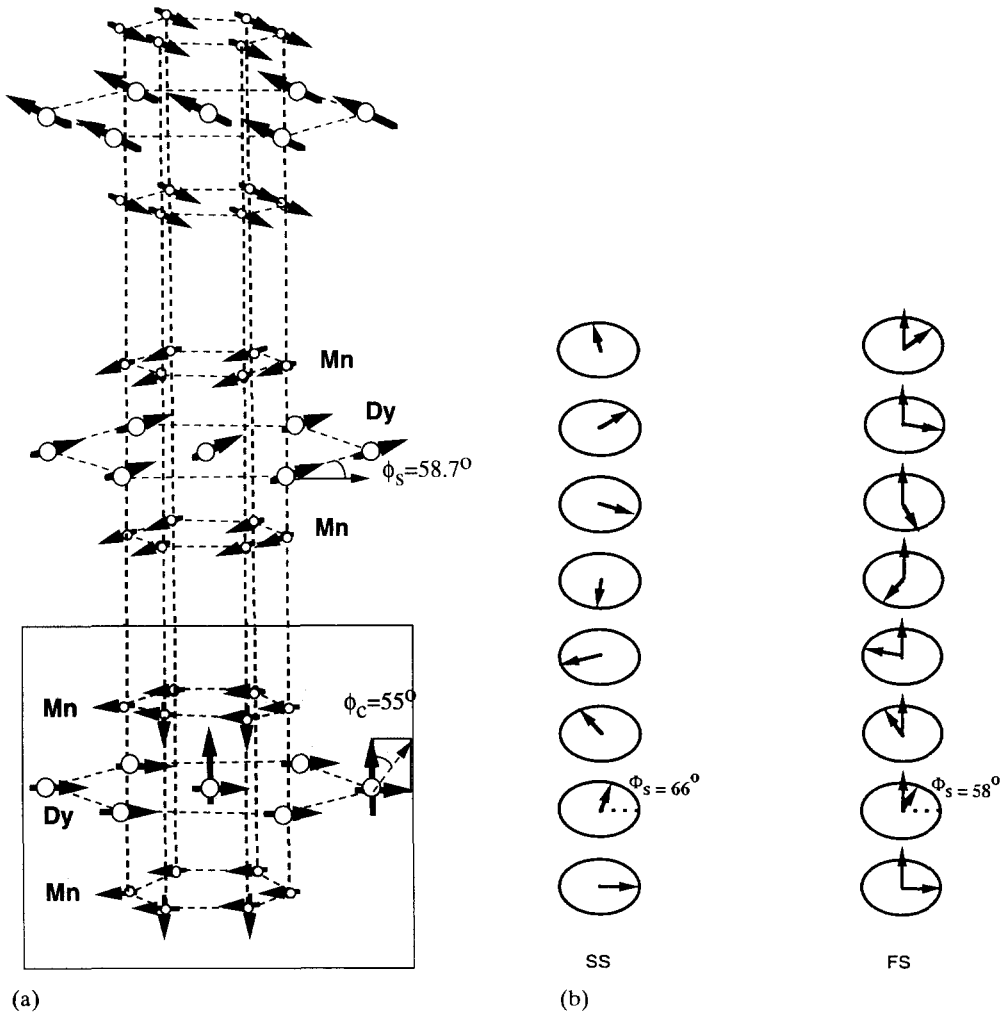


Fig. 4. (a) Schematic representation of the ferrimagnetic spiral (FS) observed for  $\text{DyMn}_6\text{Ge}_6$  at 11 K (only magnetic atoms). The  $c$  axis component for Dy and Mn is shown for some of the atoms only in the bottom part of the figure. For this reason the middle part and the top part can be taken also to represent the high temperature structure (SS), bearing in mind that  $\phi_s = 58.7^\circ$  for the FS structure and  $\phi_s = 66^\circ$  for the SS structure. (b) Schematic representation of the moment arrangement of the triple-spiral unit in  $\text{DyMn}_6\text{Ge}_6$  for the low temperature phase (FS) that has a net moment and the high temperature phase (SS) that has no net moment.

going from 293 to 11 K. Given the fact that the (001) reflection has zero magnetic contribution, the ferrimagnetic component is confined to the [001] direction.

From the refined Fourier components at 11 K associated with the wavevectors  $\pm q_z$  and  $q=0$  one may calculate the ordered moment values as a superposition of the Fourier coefficients by means of eqn. (1). Thus the resulting magnetic structure corresponds to a conical ferrimagnetic spiral (FS) as shown in Fig. 4. The magnetic moments are  $\mu_{\text{Dy}} = 6.96(8) \mu_{\text{B}}$  and  $\mu_{\text{Mn}} = -1.94(8) \mu_{\text{B}}$ . The two sublattice moments are coupled antiferromagnetically and form an angle of  $55.5(5)^\circ$  with the  $c$  axis. The net ferrimagnetic moment is along  $c$  and equals  $2 \mu_{\text{B}}$  per formula unit (f.u.). Refined parameters based on the ferrimagnetic cone structure are listed in Table 1. Observed and calculated integrated intensities can be compared with each other

in Table 3. The value of  $\chi^2$  given for the FS structure in Table 1 is still comparatively high. It is possible that this originates from the presence of higher order satellites which are less easily detected in powder data.

#### 4. Discussion

The refined  $\mu_z$  moment components  $\mu_{z\text{Dy}} = 4.02(11) \mu_{\text{B}}$  and  $\mu_{z\text{Mn}} = -1.09(8) \mu_{\text{B}}$  at 11 K contribute only to the Fourier coefficients associated with the wavevector  $q=0$ . The components within the hexagonal plane,  $\mu_{xy\text{Dy}} = 5.68(6) \mu_{\text{B}}$  and  $\mu_{xy\text{Mn}} = -1.61(2) \mu_{\text{B}}$ , contribute to the Fourier coefficients of the spiral structure,  $m_{\pm q_z}$ . In the simple spiral structure at 293 K the ferrimagnetic  $z$  component is absent, while the components within the hexagonal plane are  $3.49(8) \mu_{\text{B}}$  for Dy and  $-1.42(4) \mu_{\text{B}}$  for Mn.

TABLE 2. Some of the observed and calculated integrated neutron intensities of DyMn<sub>6</sub>Ge<sub>6</sub> at 293 K. The indexing of the magnetic ( $H \pm q_z$ ) satellites refers to  $q_z = 0.183$ 

$H K L$	$2\theta$ (deg)	$I_{\text{calc}}$	$I_{\text{obs}}$	$H K L$ $\pm q_z$	$2\theta$ (deg)	$I_{\text{calc}}$	$I_{\text{obs}}$
0 0 1	11.977	253	298	0 0 1-	9.759	515	720
1 0 0	21.697	2227	2225	0 0 1+	14.199	210	170
				0 0 2-	21.833	714	747
				{1 -1 0}±	21.811	668	698
				{1 -1 -1}±	23.839	228	242
0 0 2	24.086	4435	4548				
1 0 1	24.853	341	312	{0 1 -1}±	26.025	208	198
				0 0 2+	26.349	447	453
				{0 1 -2}±	30.972	22	48
1 0 2	32.639	561	692				
				0 0 3-	34.160	28	67
				{0 1 -2}±	34.385	22	32
0 0 3	36.477	494	607				
1 1 0	38.051	6917	6768	{1 -2 0}±	38.120	168	168
				0 0 3+	38.810	21	29
				{1 -2 -1}±	39.377	66	110
1 1 1	40.031	139	150	{0 1 -3}±	40.832	96	90
				{1 -2 1}±	40.807	62	60
1 0 3	42.841	2450	2212				
2 0 0	44.224	29	31	{1 -2 2}±	44.297	14	14
				{2 -2 0}±	44.285	18	18
1 1 2	45.541	2435	2415	{0 1 -3}±	44.896	80	62
2 0 1	45.985	111	109	{0 2 -1}±	45.401	44	48
				0 0 4-	46.910	4	11
				{1 -2 -2}-	46.877	14	24
0 0 4	49.328	62	129	{0 2 -2}+	49.843	260	308
2 0 2	50.983	446	489	0 0 4+	51.770	2	3
				{1 -2 3}±	52.053	44	50
				{0 1 -4}±	52.244	122	156
				{0 2 -2}±	52.213	234	282
1 1 3	53.732	1522	1658				
1 0 4	54.488	21	48	{1 -2 3}±	55.480	40	20

These results mean that the phase transition from the simple spiral structure to the conical ferrimagnetic spiral structure is associated with a change in the angle  $\phi_c$  of the moments with the  $c$  axis. This angle changes from  $90^\circ$  to  $55.5(5)^\circ$  on going from the high to the low temperature magnetic structure and is associated with the appearance of a net moment. The Dy and Mn sublattices order at the same temperature ( $T_N$ ) and are coupled antiferromagnetically over the whole ordered region, but have competing anisotropies and different temperature dependences of their magnetic moments.

A phase transition from a flat to a conical spiral with wavevector  $q = (0, 0, q_z)$  has also been found for the hexagonal metal Ho [12, 13]. On the basis of the Landau theory the two structures were described using the irreducible representations of the star of the vector  $q=0$  of the group  $D_{6h}^4$  at the symmetry point of the Brillouin zone. The flat spiral structure can be described

by the two-dimensional representation  $\tau_9$  in the notation of ref. 14, while the description of the conical spiral structure would need two representations,  $\tau_9 + \tau_3$ . The representation  $\tau_3$  is one dimensional and describes the ferromagnetic component along the  $c$  direction. In the hamiltonian of the flat spiral structure with a two-dimensional order parameter the anisotropy is of the order  $n=6$ . For the description of the conical spiral structure one needs two order parameters and the magnetic phase diagram for this type of transition between phases of different symmetries has not yet been clearly established.

Although the nature of this phase transition in DyMn<sub>6</sub>Ge<sub>6</sub> is not yet understood, it is interesting to note that in the collinear ferrimagnetic stannide HoMn<sub>6</sub>Sn<sub>6</sub> one observes the same moment configuration within the chemical cell as in the case of DyMn<sub>6</sub>Ge<sub>6</sub> [15]. In the former case one observes a simultaneous ordering of the two net sublattice moments that become

TABLE 3. Some of the observed and calculated integrated neutron intensities of DyMn<sub>6</sub>Ge<sub>6</sub> at 11 K. The left part of the table comprises the nuclear and ferromagnetic contributions associated with  $q = 0$ . The right part refers to the magnetic ( $H \pm q_z$ ) satellites associated with  $q_z = 0.163$

$H K L$	$2\theta$ (deg)	$I_{\text{calc}}$ nucl.	$I_{\text{calc}}$ mag.	$I_{\text{calc}}$ total	$I_{\text{obs}}$ total	$H K L$ $\pm q_z$	$2\theta$ (deg)	$I_{\text{calc}}$	$I_{\text{obs}}$
0 0 1	11.996	705	0	705	748	0 0 1-	10.034	3121	3825
						0 0 1+	13.961	1530	1050
1 0 0	21.773	6247	2979	9226	9242	{1 -1 0}±	21.862	3792	3780
						0 0 2-	22.133	3246	3242
0 0 2	24.126	12463	0	12463	12666	{1 -1 -1}±	24.025	1688	1730
1 0 1	24.930	975	1626	2601	2647	{0 1 -1}±	26.026	2182	2435
						0 0 2+	26.126	2182	2453
						{0 1 -2}±	31.243	394	446
1 0 2	32.721	1613	186	1799	1997	{0 1 -2}±	34.260	352	462
						0 0 3-	34.488	211	217
0 0 3	36.538	1414	0	1414	1633	{1 -2 0}±	38.241	978	956
1 1 0	38.188	19544	771	20315	19761	0 0 3+	38.600	162	221
						{1 -2 -1}±	39.584	490	728
1 1 1	40.168	400	648	1048	1124	{1 -2 1}±	40.847	480	584
						{0 1 -3}±	41.157	720	742
1 0 3	42.935	6372	162	6534	6324	{2 -2 0}±	44.433	4	4
2 0 0	44.385	83	0	83	119	{1 -2 2}±	44.557	172	164
						{0 1 -3}±	44.750	602	540
1 1 2	45.682	6870	156	7026	7041	{0 2 -1}±	45.624	344	352
2 0 1	46.146	351	474	789	828	{1 -2 -2}-	46.857	166	174
						0 0 4-	47.273	1	14
0 0 4	49.413	182	0	182	208	{0 2 -2}+	50.136	1286	1468
2 0 2	51.148	1252	1198	2450	2478	0 0 4+	51.571	0	0
						{0 2 -2}±	52.231	1186	1368
						{1 -2 3}±	52.393	334	338
						{0 1 -4}±	52.615	738	890
1 1 3	53.881	4341	180	4521	4880	{1 -2 3}±	55.423	298	236
1 0 4	54.601	55	96	151	254				

antiferromagnetically aligned below  $T_N = 376$  K. Below 200 K a reorientation of the magnetic moments occurs. In the high temperature region the moments lie in the (001) plane, while in the interval 180–120 K the angle between the moments and the  $c$  axis changes from  $90^\circ$  to  $49^\circ$ . In the case of DyMn<sub>6</sub>Ge<sub>6</sub>, however, the situation is more complex, since the basic structure has also become drastically modified upon cooling.

The results of the magnetic measurements shown in Fig. 1 suggest that the temperature-induced change from the spiral structure (zero net moment) to the double-cone structure (non-zero net moment) takes place at about 80 K. The spontaneous moment of DyMn<sub>6</sub>Ge<sub>6</sub> estimated from the magnetic measurements is about  $1 \mu_B/\text{f.u.}$  This is lower than the net moment of  $2.0(5) \mu_B/\text{f.u.}$  derived from the neutron results, but the result is satisfactory if one takes into account that the latter number is the difference between two large

numbers representing the  $z$  components of the Dy and Mn sublattices.

The high field measurements displayed in Fig. 2 can conveniently be interpreted on the basis of the structural information obtained from neutron diffraction. Since the net moment is along the  $c$  axis at low temperatures, the powder particles will orient themselves with their  $c$  axis pointing into the field direction. The part of the magnetic isotherm below the discontinuity (at about 22 T) is most likely due to the closing up of the cone angle  $\phi_c$ , reaching a basically antiparallel moment arrangement at about 22 T. The field at the discontinuity at about 22 T can be identified as the critical field. At higher fields the antiparallel coupling between the Dy and Mn sublattices becomes unstable and the two sublattice moments start to bend towards each other, the  $c$  axis of the particles now being turned into a direction perpendicular to the field direction. In the

linear part of the  $M(B)$  curve above 22 T one may use the relation [16]

$$\frac{dM}{dB} = \frac{1}{n_{\text{Dy-Mn}}} \quad (6)$$

to obtain the mean field coupling constant  $n_{\text{Dy-Mn}}$  between the Dy and Mn sublattice moments. The value equals  $1.13 \text{ T kg A}^{-1} \text{ m}^{-2}$  and corresponds to  $J_{\text{Dy-Mn}}/k = -9.14 \text{ K}$  for the coupling constant between a single pair of Dy and Mn spin moments in the hamiltonian  $H_{\text{ex}} = -2J_{\text{Dy-Mn}}S_{\text{Mn}} \cdot S_{\text{Dy}}$  (for more details see ref. 16). Coupling constants of similar sign and magnitude have been found for most of the many other types of intermetallic compounds of rare earth and 3d metals.

### Acknowledgment

The authors are grateful to Dr. J. Rodriguez-Carvajal for useful discussions and for the use of the FULLPROF computer program.

### References

- 1 J.H.V.J. Brabers, V.H.M. Duijn, F.R. de Boer and K.H.J. Buschow, *J. Alloys Comp.*, 198 (1993) 127.
- 2 R.R. Olenich, L.G. Akselrud and Ya. P. Yarmoliuk, *Dopov. Akad. Nauk. Ukr. RSR Ser. A*, (2) (1981) 84.
- 3 E. Parthé and B. Chabot, in K.A. Gschneidner Jr. and L. Eyring (eds.), *Handbook on the Physics and Chemistry of Rare Earths*, Vol. 6, North-Holland, Amsterdam, 1984, p. 113.
- 4 G. Venturini, R. Welter and B. Malaman, *J. Alloys Comp.*, 185 (1992) 99–107.
- 5 J. Rodriguez-Carvajal, *Abstracts of Satellite Meeting on Powder Diffraction on XVth Congr. of IUC, Toulouse, 1990*, Université Paul Sabatier, Toulouse, 1990, p. 127.
- 6 L. Koester, H. Rauch and E. Seymann, *At. Data Nucl. Data Tables*, 49 (1991) 65.
- 7 A.J. Freeman and J.P. Desclaux, *J. Magn. Magn. Mater.*, 12 (1979) 11.
- 8 A.C.C. Wilson (ed.), *International Tables for Crystallography*, Vol. C, Kluwer, Dordrecht/Boston/London, 1992.
- 9 T. Nagamiya, *Solid State Phys.*, 20 (1967) 305.
- 10 J. Rossat-Mignod, Magnetic structures, in *Methods of Experimental Physics: Neutron Scattering*, Vol. 3, Academic, New York, 1987, p. 69.
- 11 G. Shirane, *Acta Crystallogr.*, 12 (1959) 282.
- 12 W.C. Koehler, in R.J. Elliott (ed.), *Magnetic Properties of Rare Earth Metals*, Plenum, London/New York, 1972, p. 80.
- 13 Yu. A. Izyumov, V.M. Laptev and S.B. Petrov, *J. Magn. Magn. Mater.*, 44 (1984) 35.
- 14 O.V. Kovalev, *Irreducible Representations of the Space Groups*, Gordon and Breach, New York/London/Paris, 1965.
- 15 B. Chafik El Irdissi, G. Venturini and B. Malaman, *J. Less-Common Met.*, 175 (1991) 143.
- 16 R. Verhoef, R.J. Radwanski and J.J.M. Franse, *J. Magn. Magn. Mater.*, 89 (1992) 176.